

Accurate Supercapacitor Modeling for Energy-Harvesting Wireless Sensor Nodes

Alex S. Weddell, *Member, IEEE*, Geoff V. Merrett, *Member, IEEE*, Tom J. Kazmierski, *Senior Member, IEEE*, and Bashir M. Al-Hashimi, *Fellow, IEEE*

Abstract—Supercapacitors are often used in energy-harvesting wireless sensor nodes (EH-WSNs) to store harvested energy. Until now, research into the use of supercapacitors in EH-WSNs has considered them to be ideal or over-simplified, with non-ideal behavior attributed to substantial leakage currents. In this brief, we show that observations previously attributed to leakage are predominantly due to redistribution of charge inside the supercapacitor. We confirm this hypothesis through the development of a circuit-based model which accurately represents non-ideal behavior. The model correlates well with practical validations representing the operation of an EH-WSN, and allows behavior to be simulated over long periods.

Index Terms—energy harvesting, supercapacitor modeling, system simulation, wireless sensor networks, supercapacitor leakage

I. INTRODUCTION AND MOTIVATION

SUPERCAPACITORS (also known as ultracapacitors or double-layer capacitors) are commonly used in energy-harvesting wireless sensor nodes (EH-WSNs) to store harvested energy. They are attractive as they have a higher power density than batteries, do not require special charging circuitry, and have a long operational lifetime which is usually considered to be unrelated to the number of charge/discharge cycles [1]. This work focuses on modeling small supercapacitors, often found in EH-WSN applications.

While supercapacitors are commonly used in EH-WSNs, the understanding of device behavior in these applications is primitive. Some reported works have assumed that supercapacitors behave as ideal devices [2], or have used simplistic models to explain their short-term behavior [3]. Alternatively, they have directly related the leakage power [4],[5] or current [6], to the terminal voltage. Other works have suggested that the number of charge/discharge cycles does, in fact, affect the supercapacitor's leakage characteristics [7]. Supercapacitor behavior is not ideal and devices exhibit characteristics such as voltage drop and recovery, which occur over very long periods.

Manuscript received June 1, 2011, revised August 3 2011, accepted September 14 2011.

This work was supported by the Engineering and Physical Sciences Research Council (EPSRC) under grant number EP/G067740/1 "Next Generation Energy-Harvesting Electronics: Holistic Approach," website: www.holistic.ecs.soton.ac.uk

The authors are with Electronics and Computer Science, University of Southampton, UK, SO17 1BJ e-mail: {asw,gvm,tjk,bmah}@ecs.soton.ac.uk

Color versions of one or more of the figures in this paper are available online at <http://ieeexplore.ieee.org>

Copyright ©2011 IEEE. Personal use of this material is permitted. However, permission to use this material for any other purposes must be obtained from the IEEE by sending an email to pubs-permissions@ieee.org

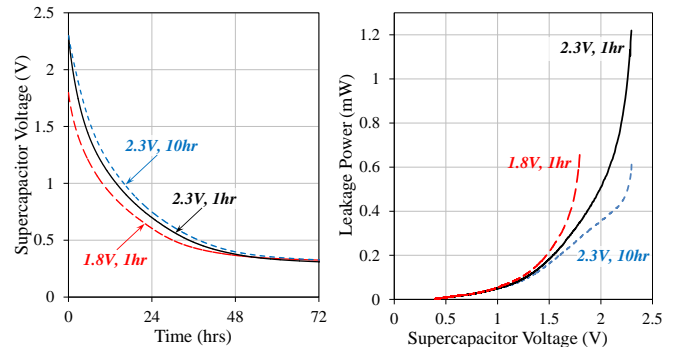


Fig. 1. (a) Experimental results obtained having charged a 4.7F supercapacitor (rated at 2.3V) to voltages of 1.8V and 2.3V, 'held' it at this voltage for 1hr and 10hrs, then monitored the open-circuit voltage across its terminals after disconnection; (b) the 'leakage power' inferred from these results (1).

Many research efforts into the use of supercapacitors in EH-WSNs attributed these non-idealities to significant leakage. Some made recommendations to keep the voltage across the supercapacitor as low as possible [8],[9]. These investigations predominantly used the same method: to illustrate this, we charged a supercapacitor to a test voltage, held it at this value for a charging period, disconnected it from the power supply, and then monitored its open-circuit voltage over time. These data were subsequently processed assuming that the energy stored can be estimated from observation of the terminal voltage and using the ideal capacitor equation $E = CV^2/2$. Hence, using (1), an effective 'leakage power' can be inferred.

$$P_l = \frac{dE}{dt} = \frac{C}{2} \cdot \frac{d(V^2)}{dt} \quad (1)$$

This experiment was performed a number of times on a supercapacitor (4.7F, rated at 2.3V). First, a test voltage of 2.3V and a charging period of 1hr were used; the measured open-circuit voltage and effective 'leakage power' are shown by the solid lines (2.3V, 1hr) in Fig. 1. From this, a roughly exponential relationship is observed between supercapacitor leakage and voltage; hence an intuitive conclusion is that because greater 'leakage' is experienced at higher voltages, supercapacitors should avoid operating in this region. However, we repeated the experiment using a lower test voltage of 1.8V (dashed lines (1.8V, 1hr) in Fig. 1), and considerably more 'leakage' was exhibited between 1-1.8V. We also repeated the original experiment, but with a longer charging period of 10hr (dotted lines (2.3V, 10hr) in Fig. 1), and less 'leakage' was observed. This range of charging periods is representative of typical energy harvesting applications, for example daily solar

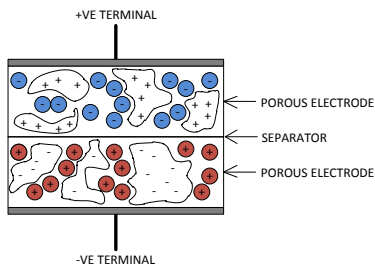


Fig. 2. Conceptual diagram showing the internal construction of a supercapacitor (also known as an ‘electric double-layer capacitor’).

cycles or intermittent wind sources [10]. These experimental results illustrate that the earlier assumptions are potentially misleading as they over-simplify the problems of leakage, and the ideal capacitor equation does not represent the supercapacitor’s non-linear, complex, and temporal behavior.

In this brief, we show that effects previously attributed to leakage are instead dominated by redistribution of charge inside the supercapacitor (Sec. II). The proposed model reflects the behavior of supercapacitors with adequate accuracy without a dedicated leakage resistor, and confirm this hypothesis through the development of a circuit-based model which accurately represents non-ideal behavior. A device has been characterized and model parameters have been generated (Sec. III), and the model has been practically validated (Sec. IV).

II. NON-IDEAL SUPERCAPACITOR BEHAVIOR AND RELATED WORK

The non-ideal characteristics of supercapacitors stem from their internal construction. Unlike conventional capacitors, the supercapacitor has two solid electrodes (in contact with a terminal plate) each with a liquid electrolyte [1]. The area between the solid electrode material and its electrolyte solution, as shown in Fig. 2, forms the ‘double layer’. Due to the fact that charge is stored across a very large effective surface area within the porous electrode, high capacitance values can be achieved in relatively small volumes.

As the charge is stored in the electrolyte, this means that extraction of charge relies on its diffusion, and therefore some processes in supercapacitors have very long time constants. Indeed, Panasonic state that it “...takes a minimum of 10 hours to fully charge the capacitor...” [1]. They also show that the charging current drops to approximately $1\mu\text{A}$ when the device has been held at a voltage for a long period – indicating the presence of an equal, and thus negligible, leakage current. The two electrodes are divided by a thin separator membrane to prevent short-circuit. The electrode construction means that the supercapacitor’s maximum operating voltage is relatively low (typically around 2.3V), after which permanent damage can occur (breakdown effects are not covered by the proposed model). Complex behavior means that some effects are mistakenly attributed to leakage and the efficiency of charging schemes is difficult to assess.

In recently-reported energy-harvesting systems, simplistic models and assumptions were used to explain the short and long-term behavior of supercapacitors. It is often assumed

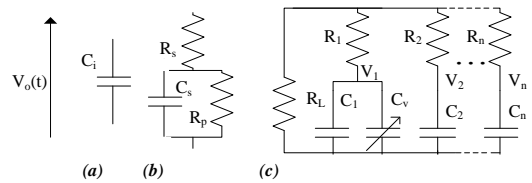


Fig. 3. Circuit-based supercapacitor models: (a) an ideal capacitor (b) simplified model including a series and parallel resistance [3] (c) RC ladder circuit with a voltage-dependent capacitance in its first branch, which may be extended to n branches [11].

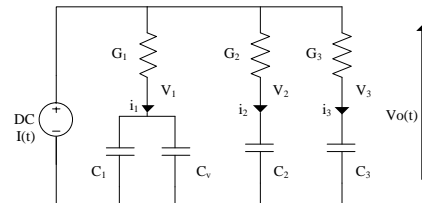


Fig. 4. Three-branch equivalent circuit, based on the RC ladder circuit from Fig. 3(c). The circuit includes a voltage-dependent capacitance term in its first branch. This equivalent circuit model is used in our work.

that supercapacitor behavior can be modeled closely as the behavior of ideal conventional capacitors (Fig. 3(a)), especially when assessing their state-of-charge [2]. Some applications attribute their voltage drop to a high self-discharge rate: e.g. a classical model (Fig. 3(b)) shows the supercapacitor as an ideal capacitance with an equivalent series resistance (ESR) and an equivalent parallel (leakage) resistance (EPR) [3].

A limited number of models have recognized the true behavior of supercapacitors: ladder circuits (Fig. 3(c)) were described by Buller *et al.* [12], which used a ladder of resistors and capacitors; however, these models were exclusively interested in the very short-term behavior of the supercapacitor, using AC impedance measurements to calculate branch parameters (in their presented model, the longest τ was <10 seconds). Perhaps the most thorough investigation into longer-term supercapacitor behavior was carried out by Zubieta and Bonert [11], which proposed a three-branch supercapacitor model and a characterization process which allowed the supercapacitor parameters to be determined automatically. Recognizing the long-duration processes within the supercapacitor, they also proposed a ‘normalization’ technique which is used to ensure that the supercapacitor is empty by accelerating the redistribution of charge within the device. However, their model made the critical simplifying assumption that each branch operates independently (e.g. while the immediate branch is charging, there is no interaction from the delayed or long branches), and was only applied to larger capacitors for power electronics applications, such as hybrid electric vehicles, rather than the smaller devices considered in this work.

III. CHARACTERIZATION AND SIMULATION APPROACH

The starting point for our supercapacitor characterization methodology is that described by Zubieta and Bonert [11], which reported very good levels of accuracy for modeling large capacitors over short time periods. Unlike the reported

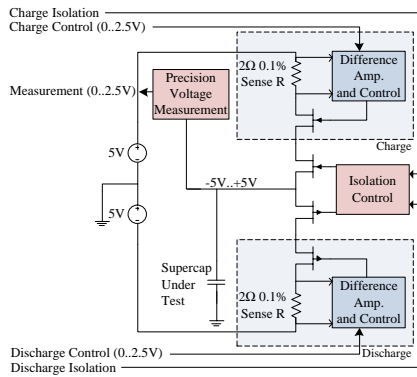


Fig. 5. Circuit used for test of supercapacitor behavior.

work, the new method we have developed does not assume that branches act independently, using a new way of calculating the equivalent circuit parameters, thus allowing a wider range of time periods to be simulated. From here on, the model we use will have three branches (Fig. 4) and, for conciseness, only equations for 3-branch models are considered as we found that it gives a suitable level of accuracy for the supercapacitor and time periods considered in this study (from seconds up to a few hours). However, the process of extending the model and method to four or more branches is trivial, so supercapacitor performance over even longer periods could be modeled. As with the previously-reported model [11], our model includes a voltage-dependent capacitor in the first branch to represent the non-linear behavior of the device which has been observed in practice. The use of multiple branches enables the long-term charging process to be modeled, which is dependent on the physical distribution of charge within the electrode.

A test system has been developed which allows the supercapacitor to be normalized and subjected to controlled-current tests which then enable the equivalent circuit parameters to be calculated. The test circuit shown in Fig. 5 was implemented (Fig. 6), and is capable of subjecting the supercapacitor under test to controlled-current charge and discharge. It has been developed to deliver a range of voltages and currents and hence is capable of characterizing the range of supercapacitors used in EH-WSNs. It is able to charge or discharge at up to 250mA in 1mA increments and current values are stable within 2ms. It is managed by a control algorithm implemented on an MSP430FG4618 microcontroller (Fig. 6), which actions the normalization and charge/discharge profiles required by the test procedure. The microcontroller interfaces with a PC serial port, with the PC acting as a data logger. The circuit control voltages are between 0..2.5V and are each controlled by a DAC output from the MSP430. The precision voltage measurement circuit implements a high-impedance buffer arrangement which brings the -5V..+5V measurement range into the 0..2.5V range for input to the MSP430 ADC. A precision 2.5V reference was used to improve the ADC accuracy, and a crystal was added to the board for precision timing.

The characterization process for the supercapacitor involves normalization over a 24-hour period before commencement of the test [11]. The test was initialized with a rapid charge (at 100mA) from zero volts to the maximum rated voltage of the

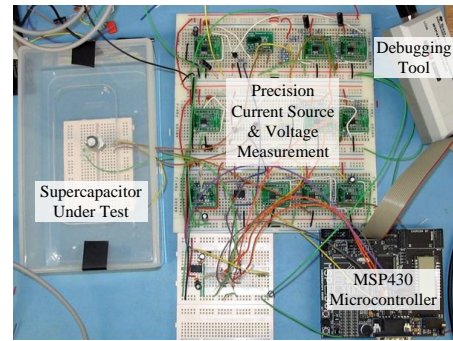


Fig. 6. The test set-up, including the supercapacitor under test, the test circuitry on prototype board, and the interface and control functionality provided by an MSP430 microcontroller.

device. The charge was then terminated, and the supercapacitor left in open-circuit for one hour. A gradual discharge (at 10mA) then followed, with the discharge terminated at 1.0V. The device was then left in open-circuit for several hours. This sequence was to enable the performance of the capacitor under rapid and gradual charge/discharge conditions to be modeled, with the long open-circuit times allowing the dynamics of slow charge redistribution to be observed.

To deliver control over the simulation process it was decided to pursue a state variable-based simulation technique [13], which was implemented in MATLAB. Through use of the `ode45` differential equation solver and the segmentation of the simulation into distinct sections (charge, charge relaxation, discharge, discharge relaxation) the simulation behavior in transition areas was improved. State equations (2)–(5) were formulated from the three-branch equivalent circuit (Fig. 4), but with resistors substituted for conductances, and allow the circuit operation to be simulated effectively. Equation (2) includes the voltage-dependent capacitor C_v , used by Zubietta and Bonert [11], which represents the non-linear behavior that is particularly evident in the shape of the charging curve.

$$\alpha = \left(C_1 + \frac{C_v \cdot v_1}{2} \right) \quad (2)$$

$$\alpha \cdot v_1 = G_1 \cdot \frac{I + G_2(v_2 - v_1) + G_3(v_3 - v_1)}{G_1 + G_2 + G_3} \quad (3)$$

$$C_2 \cdot \dot{v}_2 = G_2 \cdot \frac{I + G_1(v_1 - v_2) + G_3(v_3 - v_2)}{G_1 + G_2 + G_3} \quad (4)$$

$$C_3 \cdot \dot{v}_3 = G_3 \cdot \frac{I + G_2(v_2 - v_3) + G_1(v_1 - v_3)}{G_1 + G_2 + G_3} \quad (5)$$

The three-branch model (Fig. 4) was used as it delivers an effective balance between computational effort and accuracy (for the time period studied in this work) and was used in earlier reported works [11]. The first branch represents the ‘fast’ response of the supercapacitor, and the subsequent branches model the ‘intermediate’ and ‘long’ responses. The branches have correspondingly time constants, and model the experimentally-observed physical effects of redistribution of charge within the supercapacitor under charge/discharge (Sec. II), with the physical causes being explained by the manufacturer [1]. A genetic optimization algorithm was used,

TABLE I
EXPERIMENTALLY-OBTAINED PARAMETER VALUES FOR 3-BRANCH
MODEL OF PANASONIC GOLD 4.7F SUPERCAPACITOR

Component	Value
C_v	0.945 F/V
C_1	2.62 F
C_2	1.45 F
C_3	3.88 F
R_1	0.178 Ω
R_2	94.2 Ω
R_3	1030 Ω

TABLE II
PARAMETER VALUES FOR IDEAL AND SIMPLIFIED MODELS OF
PANASONIC GOLD 4.7F SUPERCAPACITOR

Component	Value
C_i	4.7 F
C_s	4.06 F
R_s	0.80 Ω
R_p	2.01 k Ω

which bypasses the necessary assumption of previous works that there was no interaction between branches during rapid charge or discharge. The optimization process was initialized to deliver a 10x separation of time constants between each branch. The optimization variables enable the time constant and capacitor size of each branch to be optimized, effectively allowing the R and C values to be set independently while maintaining a separation between the branch time constants.

The MATLAB genetic optimization algorithm was used to fit the simulated behavior to the experimental data obtained under the characterization test. A cost function was defined, with points linearly distributed through each of the the charge, discharge, and relaxation curves. The 3-branch model optimization involved a total of 7 variables ($x_1 \dots x_7$). Variable x_1 defines C_v , and x_2 to x_4 define C_1 to C_3 . The time constants of the second and third branches τ_2 and τ_3 , are set by x_5 and x_6 . The value of R_1 was adjusted using x_7 . The genetic optimization was initialized using reasonable upper and lower bounds and an initial population of 100.

IV. EXPERIMENTAL VALIDATION

A Panasonic Gold 4.7F supercapacitor was characterized using the above method. To verify the model parameters, a test tailored to an EH-WSN was carried out. We ran simulations of a charge and pulsed discharge using the proposed model and the ideal and simplified models (Fig. 3), which were then compared against the behavior of a real supercapacitor. The results of the characterization process for a 4.7F Panasonic Gold supercapacitor are shown in Table I. The ideal and simplified parameters are shown in Table II. The ideal parameter assumes the capacitance value is that rated by the manufacturer. The simplified parameters use real experimental values, with the capacitance value being derived from the charging current and time, the series resistance from the voltage increase on commencement of charge, and the parallel resistance from the voltage drop after the first hour.

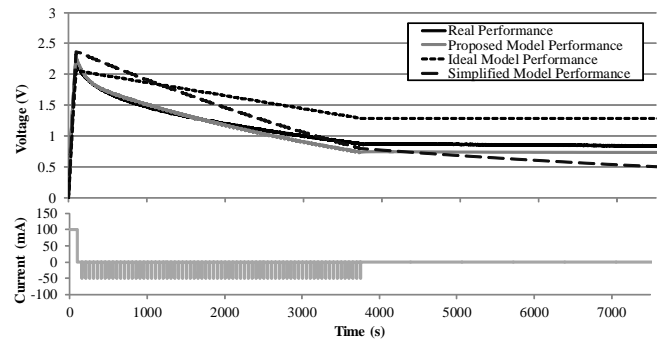


Fig. 7. The terminal voltages from each model (ideal, simplified and proposed) and experimental results for the pulsed discharge (typical in EH-WSNs) of a 4.7F supercapacitor.

Firstly, to remove any residual charge from the supercapacitor, the supercapacitor under test was normalized for 24 hours. Next, it was rapidly charged at 100mA. This charging current allowed the verification of both the ‘fast’ and ‘slow’ effects of the supercapacitor behavior to be verified, and is consistent with the charging rate of the supercapacitor in, for example, the Prometheus mote [2] (a solar EH-WSN which reduces stress on a rechargeable battery by transferring energy to and from a supercapacitor). After charging, the supercapacitor was rested for one minute before entering a pulsed discharge test for one hour. The device was subjected to a pulsed discharge of 50mA with a 2% duty cycle (50mA discharge current for 1s and open circuit for 49s). This discharge current pattern is realistic and consistent with typical wireless sensor nodes. After completion of the one-hour test, the device was left in open-circuit for a further hour. The voltage was logged at least once per second throughout the execution of this test.

This charge/discharge pattern was also used in simulation (with the parameters given in Table I), and a comparison showing the supercapacitor terminal voltage for the experimental and modeled tests is shown in Fig. 7. There is a good correlation between the real (solid black line) and proposed (solid gray line) model performance, indicating that the generated model and parameters are correct for an EH-WSN. The voltage curves for the other models (Fig. 3) are also shown. Both the shape and the absolute values obtained from these simpler models display considerable divergence from experimental performance. The assumption by the simplified model that self-discharge over the first hour is representative of the device performance causes excessive voltage drop later in the test, and the absence of a non-linear term causes the shape of the line during the pulsed discharge to be completely straight. We suspect that the small offset between the proposed model and experimental performance may be explained by the lack of voltage-dependent capacitances in the second and third branches, and is being addressed in future work.

The verified model also allows the amount of energy stored in the supercapacitor to be quantified. Fig. 8 shows the voltage across each branch of the equivalent circuit model. Fig. 9 shows the energy stored in each branch (dashed, dotted, and solid black lines), and the total energy stored across all branches (solid gray line). These figures show the voltage

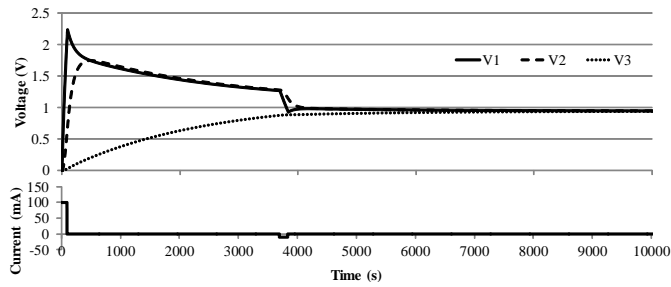


Fig. 8. The voltage across the capacitor in each branch of the proposed supercapacitor model (Fig. 4) during controlled-current characterization test.

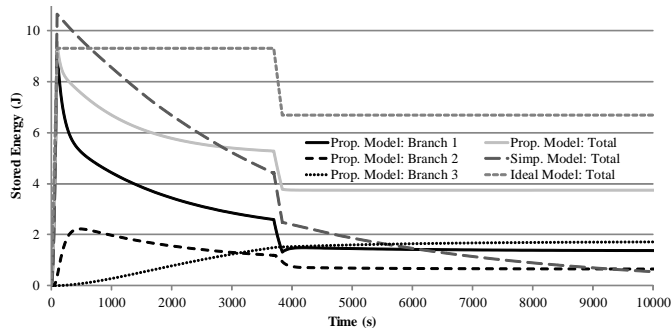


Fig. 9. The modeled energy stored in the supercapacitor for each model (ideal, simplified (Fig. 3) and proposed (Fig. 4) during controlled-current characterization test. Current profile is same as Fig. 8.

and energy dynamics during the characterization process. The figures for the proposed model show that a substantial amount of energy is lost immediately after charging is completed; this is due to the transfer of energy from branch 1 to branches 2 and 3, and not due to leakage (i.e. across the separator membrane) per se. Leakage is not explicitly modeled because, as discussed earlier, the actual leakage current is negligible (this is verified by the agreement between the modeled and real performance).

Lastly, we compare the estimates of the amounts of energy remaining in the supercapacitor for each of the models (Fig. 3) in Fig. 9. There is a large difference between the total amounts of energy estimated by each model. This is due to the continued loss of charge due to the leakage resistor in the simplified model, and the absence of any redistributive processes in the ideal model. Each of these simplified models give an inaccurate impression of the total amount of energy stored in the device, and would cause misleading conclusions to be drawn about the system performance. The solid gray line shows the total stored energy in our proposed model, and allows energy loss during charge/discharge to be inferred. The energy dissipated during charge redistribution is lost during the transfer of charge between the capacitors in each branch, passing through their associated resistors (Fig. 4).

V. CONCLUSION

The described work accurately models real-world supercapacitor operation and has a number of important implications for the design of low-power energy-harvesting systems. The simplistic assumptions of previous works have been demonstrated to be incorrect, and the presented model explains

the causes of the divergent time-sensitive behavior of the supercapacitor. Voltage changes on the terminals of the device, which are often simply attributed to leakage (shown in Fig. 1), are instead shown to be dominated by the redistribution of charge within the device, and its long time-constant processes.

The shortfalls in earlier works are due to the assumption that supercapacitor behavior is similar to that of conventional capacitors; in fact, its internal processes occur over very long time periods, which explains why charging the device for an extended period of time results in a smaller voltage drop (which is often attributed to a lower leakage power, e.g. the dotted line in Fig. 1). Many of the earlier works also made recommendations for charging strategies which have been shown to be unsound. The presentation of a circuit-based model, and a flexible optimization process which delivers model parameters, allows the supercapacitor to be modeled accurately over several hours and the stored energy to be calculated. This capability will contribute to the effective simulation and design of future EH-WSN systems.

ACKNOWLEDGMENT

The authors would like to thank Leran Wang for his assistance with MATLAB simulation.

REFERENCES

- [1] Panasonic Industrial Company, "Gold Capacitors Technical Guide," <http://www.panasonic.com/industrial/electronic-components/capacitive-products/gold-cap-electric.aspx>, 2005, last accessed May 2010.
- [2] X. Jiang, J. Polastre, and D. Culler, "Perpetual environmentally powered sensor networks," in *Proc. Int. Symp. Inform. Process. in Sensor Networks*, 2005, pp. 463–468.
- [3] D. Cahela and B. Tatarchuk, "Overview of electrochemical double layer capacitors," in *Proc. Int. Conf. Electron., Control and Instrumentation*, vol. 3, 1997, pp. 1068–1073.
- [4] C. Renner, J. Jessen, and V. Turau, "Lifetime prediction for supercapacitor-powered wireless sensor nodes," *Proc. 8th GI/ITG KuVS Fachgespräch 'Drahtlose Sensornetze'*, pp. 55–58, 2009.
- [5] G. Merrett, A. Weddell, A. Lewis, N. Harris, B. Al-Hashimi, and N. White, "An empirical energy model for supercapacitor powered wireless sensor nodes," in *Proc. Int. Conf. Comput. Commun. and Networks*, 2008, pp. 1–6.
- [6] S. Mahlke and M. Roetzer, "Energy supply considerations for self-sustaining wireless sensor networks," in *Proc. European Workshop Wireless Sensor Networks*, 2005, pp. 397–399.
- [7] D. Brunelli, C. Moser, L. Thiele, and L. Benini, "Design of a solar-harvesting circuit for batteryless embedded systems," *IEEE Trans. Circuits Syst. II, Exp. Briefs*, vol. 56, no. 11, pp. 2519–2528, 2009.
- [8] T. Zhu, Z. Zhong, T. He, and Z.-L. Zhang, "Energy-synchronized computing for sustainable sensor networks," *Ad Hoc Networks*, vol. In Press, p. 13, 2011. [Online]. Available: <http://www.sciencedirect.com/science/article/pii/S157087051000168X>
- [9] T. Zhu, Y. Gu, T. He, and Z.-L. Zhang, "eshare: a capacitor-driven energy storage and sharing network for long-term operation," in *Proc. ACM Conf. Embedded Networked Sensor Syst.*, ser. SenSys '10. New York, NY, USA: ACM, 2010, pp. 239–252.
- [10] C. Park and P. Chou, "Ambimax: Autonomous energy harvesting platform for multi-supply wireless sensor nodes," *3rd Ann. IEEE Commun. Soc. Conf. on Sensor and Ad Hoc Commun. and Networks*, vol. 1, pp. 168–177, 2006.
- [11] L. Zubieta and R. Bonert, "Characterization of double-layer capacitors for power electronics applications," *IEEE Trans. Ind. Appl.*, vol. 36, no. 1, pp. 199–205, 2000.
- [12] S. Buller, E. Karden, D. Kok, and R. De Doncker, "Modeling the dynamic behavior of supercapacitors using impedance spectroscopy," *IEEE Trans. Ind. Appl.*, vol. 38, no. 6, pp. 1622–1626, 2002.
- [13] L. Wang, T. Kazmierski, B. Al-Hashimi, A. Weddell, G. Merrett, and I. A. Garcia, "Accelerated simulation of tunable vibration energy harvesting systems using a linearised state-space technique," in *Proc. Design, Automation and Test in Europe*, 2011, pp. 1267–1272.